ELSEVIER

Journal of Photochemistry and Photobiology A: Chemistry 109 (1997) 39–46

Journal of PHOTOCHEMISTRY AND PHOTOBIOLOGY A:CHEMISTRY

Photoelectrochemical studies on electrodes coated with polymer-bound porphyrin systems

E. Balasubramaniam [a], P. Natarajan [a,b,*]

[a] *Photochemistry Division, Central Salt and Marine Chemicals Research Institute, Bhavnagar-364002, India*

[b] *Department of Inorganic Chemistry, School of Chemistry, University of Madras, Madras-600025, India*

Accepted 17 March 1997

Abstract

Chemically modified thin film electrodes were prepared by the electropolymerization technique using zinc(II) 5-(4′-hydroxy)phenyl-10,15,20-triphenylporphine and anthraquinone-2-(1-pyrrole) monomers. The ground and excited state properties of the zinc porphyrin were examined by steady state absorption and emission spectroscopy in order to determine the type of interaction between the different dye molecules present in the polymeric thin films. Photoelectrochemical cells were constructed using polymer–dye-coated electrodes, and the response to light was investigated in air-equilibrated and deaerated conditions. The photopotential, photocurrent, action spectra and *i–V* curves were recorded. In addition, the activation energy parameters for charge migration were calculated. A mechanism is proposed for the reaction of molecular oxygen at the electrode with the photogenerated species. The migration of the photogenerated charge carriers in different modified electrodes and the role of quinone are discussed. © 1997 Elsevier Science S.A.

Keywords: Copolymer; Modified thin film electrodes; Photoelectrochemical properties; Polymer–porphyrin; Sandwich polymer

1. Introduction

Chemically modified thin film electrodes have been investigated for potential applications as chemical sensors [1], microelectronic devices [2], photoconductors [3] and in energy conversion [4–7]. Chemically modified electrodes have assumed great importance due to the need to improve the photoresponse of wide-bandgap semiconductors. In particular, porphyrins and phthalocyanines have been investigated for the development of chemically modified electrodes because of their structural resemblance to the chromophores in the photosynthetic system. The immobilization of reagents onto electrodes has been carried out [8] by several methods, including covalent bonding between reagent and electrode, chemisorption and electropolymerization. Of the coating methods, electropolymerization has been a subject of considerable interest in recent years [9], and the electrode morphology has been varied in order to achieve the desired physicochemical properties by altering the polymerization conditions.

In a chemically modified electrode [10], the active component performs an elementary act or a sequence of elementary acts directly related to the desired function, as in the case of porphyrins and polypyridyl complexes, and is also involved in a specific process, such as energy transfer, electron transfer, photoisomerization and other light-induced functions. Perturbing components, such as quenchers or a second chromophore, are used to modify the properties of the active components, and the connecting components, such as polymers, are used to link together the active components in a desired spatial arrangement. Only stable devices can process a large number of photons and thus be useful for practical applications, and hence the most desired property of any modified electrode is its chemical stability. In principle, the same photoexcited reactant can be used as oxidant and reductant, if it is both oxidizable and reducible under the conditions of the photoelectrochemical (PEC) cell. Many dyes have been used as sensitizers in PEC cells, including thionine and phenosafranine on a platinum electrode [7], alizarin and rhodamine B on TiO_2 [11] and bipyridyl complexes of Ru(II), chlorophyll and their analogues on SnO_2 [5]. More recently, polymeric porphyrin films [12] and porphyrins mixed with various pigments [13,14], such as quinone derivatives or thionines, have been used because of their partial reproducibility of the conditions in natural systems. In this investigation, we describe the spectral and PEC characteristics of polymer–porphyrin-coated indium tin oxide (ITO) electrodes.

* Corresponding author.

PII S1010-6030(97)00111-1

2. Experimental details

Pyrrole, tetrabutylammonium tetrafluoroborate, platinum wire (0.5 mm diameter) and 2-aminoanthraquinone were purchased from Aldrich, USA and were used as received. ITO-coated glass plates (CONDUCTIN 0004 A; sheet resistance, $4 \pm 0.4\ \Omega$; average of 80% light transmittance in the 450–650 nm region) were obtained from Balzers, Switzerland. Purifications of common organic solvents were carried out by standard procedures [15]. The monomers zinc(II) 5-(4′-hydroxy)phenyl-10,15,20-triphenylporphine (ZnPOH) and anthraquinone-2-(1-pyrrole) (AQP) were prepared by following the procedure given in Ref. [16]. All other chemicals were of analytical reagent grade and were used as received. Doubly distilled water was used in all the experiments.

Electrochemical polymerization was carried out using a PAR model 173 potentiostat/galvanostat by producing a cyclic triangular wave of potential from a PAR model 175 universal programmer. The current output was monitored using a PAR model 174 A polarographic analyser. A three-electrode assembly of an EG&G PAR 303 cell system, consisting of an ITO (dimensions, 1 cm × 2.5 cm) working electrode, a platinum wire auxiliary electrode and a saturated calomel electrode (SCE) reference electrode, was used. The cyclic voltammograms were recorded using a Houston Instruments (model RE 0089) *X–Y* recorder by feeding the linear sweep voltage of the working electrode to the *X* axis and the current changes at the working electrode to the *Y* axis. The electrolytic solutions were deoxygenated thoroughly with argon.

Absorption spectral measurements were carried out using Shimadzu UV–visible spectrophotometers (models UV-160 and PC 3101). Emission and excitation spectra were recorded using a Perkin–Elmer LS-50B (with fluorescence data manager software, revision 2) or a Hitachi 650-40 spectrofluorometer. The emission and excitation spectra of thin films were measured by keeping the thin film-coated glass plates on a solid mount accessory. Maximum excitation slit width and minimum emission slit width were maintained in order to capture the fluorescence without interference from scattered light. Corrections for the emission spectra were carried out by a post-run with an OBEY program which uses a correction factor curve generated relative to the standard quinone sulphate spectrum.

The PEC experiments were carried out on the modified ITO electrodes. The electropolymerized thin film coatings covered an area of about 2 cm^2 per side on ITO with a net light exposed area of 4 cm^2. The coated electrodes were stored in the dark and the film stability was checked spectrophotometrically before and after photocurrent measurements. The photogalvanic properties of the electropolymerized thin film electrodes were studied using the following two types of cell.

1. Single compartment cell. The photoelectrochemistry set-up for a single compartment cell consists of two coated ITO electrodes connected through platinum wire fused to a glass tube. The electrical contacts from the electrodes were made through mercury kept in the glass tube. The two electrodes were separated from each other by approximately 5 mm and were immersed in a suitable electrolytic solution.
2. Double compartment cell. The double compartment cell consists of two rectangular cells made of Pyrex glass connected by a sintered disc. The position of the electrodes was maintained as in the previous case with one of the compartments illuminated whilst the other was kept in the dark. The temperature of the cells was maintained by circulating water, the electrolytic solution was mixed by stirring and the cell was allowed to equilibrate at constant temperature for about 10 min before each experiment.

All PEC measurements were carried out in 1 mM potassium ferrocyanide ($K_4[Fe(CN)_6]$) in water as the electrolyte and the solution was deaerated by passing argon for 40 min when required. An argon atmosphere was maintained in the cell(s) during measurements by blowing a stream of argon at the solution interface. The light source for irradiation was a 150 W halogen lamp and the photopotential and current measurements were carried out using a digital voltmeter and digital picoammeter (model DPM 011, Scientific Instruments Ltd.) with a maximum input impedance of 2.5 kΩ. The photocurrents at different applied voltages were measured using a PAR electrochemical system. The potential was applied between the reference electrode (SCE) and the thin film electrode, and the difference between the current flows under dark and illuminated conditions at a particular applied potential gives the photocurrent at that potential. Action spectra were recorded using a monochromator (Oriel Corporation, USA) to select the wavelength. The experiments were repeated at least six times to confirm the reproducibility of the results.

3. Results and discussion

Scanning tunnelling microscopic studies [17] on an ITO electrode have revealed the surface roughness properties with an average oriented grain diameter of 16 nm and height of 6 nm. The ITO electrode was chosen for electrical and PEC studies because of its high electrical conductivity and transparency in the visible region. Thin films of ZnPOH and AQP on the ITO electrodes were obtained by the electropolymerization technique as described in Ref. [16]. Three types of polymeric thin film, namely polymer–porphyrin (P1), sandwich polymer (S1) and copolymer (C1), were obtained on ITO electrodes (Scheme 1; 1, 2 and 3 represent the ITO surface, ZnPOH and AQP respectively) and are used in this study.

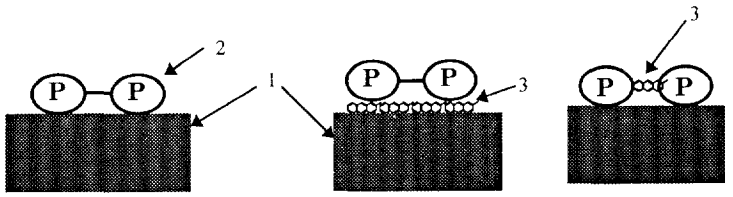

Scheme 1.

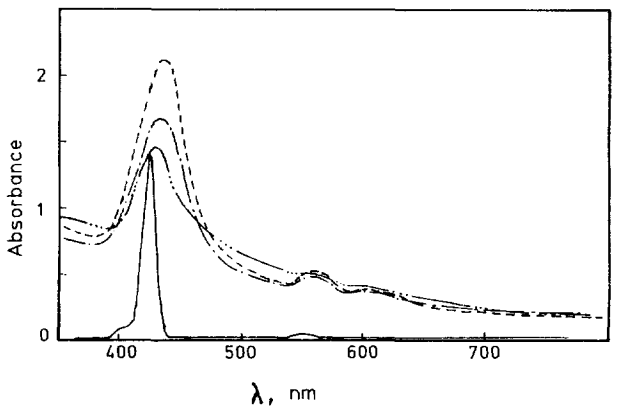

Fig. 1. Absorption spectra of ZnPOH in benzene (———) and ZnPOH on modified thin film electrodes: P1 (– – –); S1 (– · –); C1 (– · · · –).

The thickness of the thin films was estimated to be 20 ± 1 nm from the integrated current obtained for the electropolymerization process by taking into account the shape and size of the porphyrin macrocycle [16,18]. It is assumed that the thin film layer on the electrode is uniform and smooth. The UV–visible absorption spectrum of the polymeric thin film on the electrode indicates the characteristic bands due to the chromophore (see below), and the transmittance in the other regions is similar to that of an uncoated electrode.

3.1. Absorption and emission spectra of polymer–dye films

The electronic absorption spectrum (Fig. 1) of the ZnPOH monomer in benzene shows a characteristic Soret band at 428 nm ($\epsilon = 5.41 \times 10^5$ M^{-1} cm^{-1}) and Q bands at 563 nm ($\epsilon = 2.09 \times 10^4 M^{-1} cm^{-1}$) and 604 nm ($\epsilon = 1.12 \times 10^4 M^{-1}$ cm^{-1}). In the case of thin film-coated electrodes, the bands corresponding to ZnPOH are broad and red shifted by 5–10 nm (Table 1). The electrodes containing P1, S1 and C1 thin films (Scheme 1) show electronic transitions similar to those observed for monomeric ZnPOH in benzene, indicating that the porphyrin centres in the thin films have essentially electronically decoupled ground states [19]. The small red shift observed for the thin films formed by covalent linkage of ZnPOH can be attributed to the increased π conjugation resulting in a decrease in the π–π^* energy gap. In the case of the monomeric unit, the electronic transitions are explained by single point dipoles. In the polymeric films, the array of monomer units results in a band of electronic states, leading to a change in the characteristics of the relaxation phenomena and a broadening of the Soret and Q bands in the thin film-coated electrodes. Indeed, such shifts and broadening of the bands were observed by Lin et al. [20] in the case of highly conjugated acetylenyl bridged porphyrins. The full width at half-maxima (FWHM) of the intense, high-energy Soret transitions of ZnPOH in benzene and of P1, S1 and C1 thin films on ITO electrodes are summarized in Table 1. The FWHM value observed for the monomeric porphyrin in benzene is comparable with that reported [20] (747 cm^{-1}) for zinc tetraphenylporphyrin in chloroform. The thin film-coated electrodes, in general, have larger FWHM than monomeric ZnPOH in solution. Of the thin film-coated electrodes, C1 has a lower FWHM than P1 and S1. This effect is presumably due to the varying degree of interaction between the porphyrin units. In the case of the C1 thin film, simultaneous polymerization of ZnPOH and AQP yields covalently attached AQP moieties between porphyrin units, whereas in S1 or P1 thin films, ZnPOH polymerization occurs either over the poly(AQP) film or the porphyrin itself (Scheme 1). The differences in the red shifts and FWHM can be explained by the fact that, in P1 and S1 thin films, ZnPOH has an extended conjugation and vibronic coupling occurs with a similar porphyrin moiety having a 42 π-electron system, whereas, in C1

Table 1
Absorption and emission spectral characteristics of the modified electrodes

Sample	In/on	Absorption maxima [a] (nm)	FWHM [b] (cm^{-1})	Emission maxima [c] (nm)	Excitation maxima [d] (nm)
ZnPOH	Benzene	430, 563, 604	945	598, 644	–
P1	ITO	434(b), 564(b), 606(b)	2451	595	437
S1	ITO	437(b), 561(b), 602(b)	2573	595	435
C1	ITO	433(b)	1588	595	439

[a] (b), broadness of the peak.
[b] FWHM is measured for the intense Soret band.
[c] λ_{ex} is the Soret band.
[d] Excitation spectra were recorded by monitoring the fluorescence in the 600 nm region.

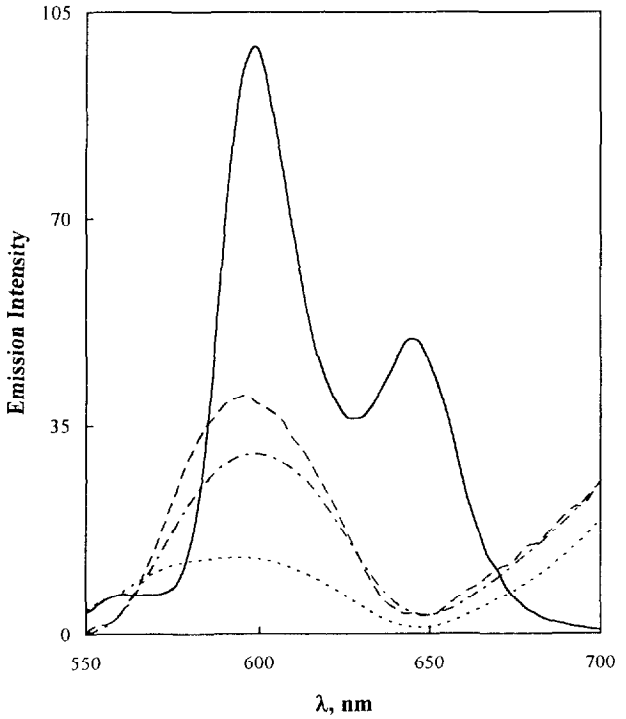

Fig. 2. Corrected emission spectra of ZnPOH in benzene (———) and ZnPOH on modified thin film electrodes: P1 (– · –); S1 (– – –); C1 (· · ·); λ_{ex}, Soret band.

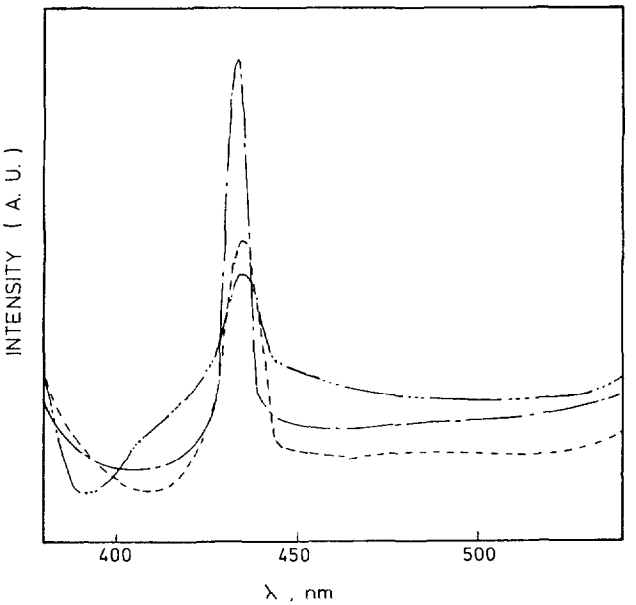

Fig. 3. Excitation spectra of ZnPOH on modified thin film electrodes: P1 (– – –); S1 (– · –); C1 (– · · · –); fluorescence was monitored at around 650 nm.

thin films, ZnPOH conjugates with the AQP moiety having only an 18 π-electron system.

The emission spectra of monomeric ZnPOH in solution and ZnPOH in polymeric thin films on ITO electrodes, on excitation of the porphyrin in the Soret band region, are shown in Fig. 2; emission bands occur at 598 and 644 nm respectively, which can be attributed to $S_1 \rightarrow S_0$ emission from the porphyrin [19]. The thin film-coated electrodes with porphyrins show only a single emission band at around 595 nm (Table 1). In addition, a considerable decrease in the fluorescence intensity of the polymerized porphyrin in the thin film electrodes is observed compared with that of monomeric ZnPOH in benzene. The decrease in the fluorescence intensity is suggested to be due to the following:

1. strong π–π electronic interaction between covalently linked porphyrins;
2. the presence of a quinone moiety, which is a strong oxidant of porphyrin excited states;
3. the formation of an exciplex or excimer.

The relative ease of exciplex formation between excited ZnPOH and electron acceptors is, among other things, a function of the electron affinity of the acceptor and the ionization energy of the excited ZnPOH. The oxidizing and reducing power of ZnPOH increases significantly on excitation, which leads to the formation of exciplexes with electron donors and acceptors (porphyrin or quinone). Although exciplex or excimer formation between excited ZnPOH and an electron acceptor is possible on the basis of energetics, the excitation (Fig. 3) and emission (Fig. 2) spectra do not support the formation of the complex. On the basis of the above reasoning, we propose that the decrease in the fluorescence intensity is due to direct energy or electron transfer processes only and not to the formation of an exciplex or excimer.

3.2. Photogalvanic cells using polymer–porphyrin-modified electrodes

Photogalvanic cells using electropolymerized thin film electrodes (two-electrode double compartment or single compartment cells) were constructed with the following (P–P) cell configuration

ITO(P2)/Fe(II) // Fe(III)/ITO(P1)

where P2 is the illuminated electrode and P1 is the dark electrode. The irradiation of P2 immersed in 1 mM $K_4[Fe(CN)_6]$ electrolytic solution leads to photocurrent generation. The evolution of the photocurrent with time is shown in Fig. 4(a) and Fig. 4(b). The open-circuit potential (ΔE_{oc}) and short-circuit photocurrent (I_{sc}) were measured under both air-equilibrated and deaerated conditions by varying the temperature from 298 to 318 K. The photovoltaic characteristics of the P–P cells at 298 K are presented in Table 2. The photocurrent and photopotential shown in Fig. 5 and Table 2 imply that charge migration takes place by two different pathways which are dependent on the concentration of dissolved oxygen in solution. In deaerated solution, P2 acts as an anode and the cell reactions are depicted below.

At the illuminated electrode

$$P2 \rightarrow P2^* \quad (1)$$

$$P2^* \rightarrow P2^{\cdot -} + e^- \quad (2)$$

$$P2^{\cdot +} + Fe^{2+} \rightarrow P2 + Fe^{3+} \quad (3)$$

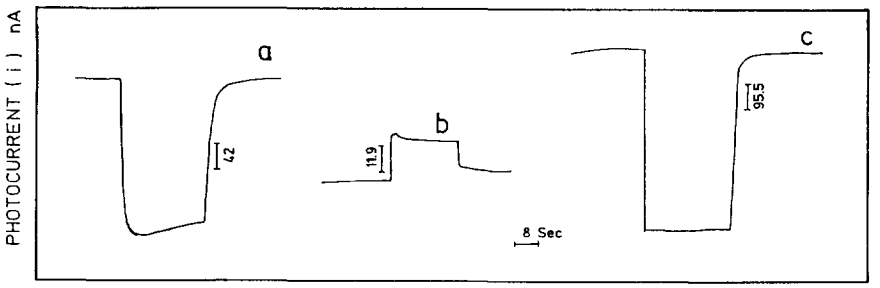

Fig. 4. Photocurrent–time response curves for P–P cells (air-equilibrated (a); deaerated (b)) and S–P cell (air-equilibrated (c)).

Table 2
Photovoltaic characteristics of modified electrodes [a]

Cell	Single compartment				Double compartment			
	Air-equilibrated solution		Deaerated solution		Air-equilibrated solution		Deaerated solution	
	ΔE_{oc} (mV)	I_{sc} (nA)	ΔE_{oc} (mV)	I_{sc} (nA)	ΔE_{oc} (mV)	I_{sc} (nA)	ΔE_{oc} (mV)	I_{sc} (nA)
P–P	−45.9	−25	41.5	38	−157	−22.7	49.0	19.0
S–P	−163	−410	16.2	12.5	−253	−649	6.6	27.0
C–P	−79.7	−177	114	66	−163	−91	119	87.5

[a] Each value is the average of at least six readings. The maximum variation in ΔE_{oc} and I_{sc} is less than 2%.

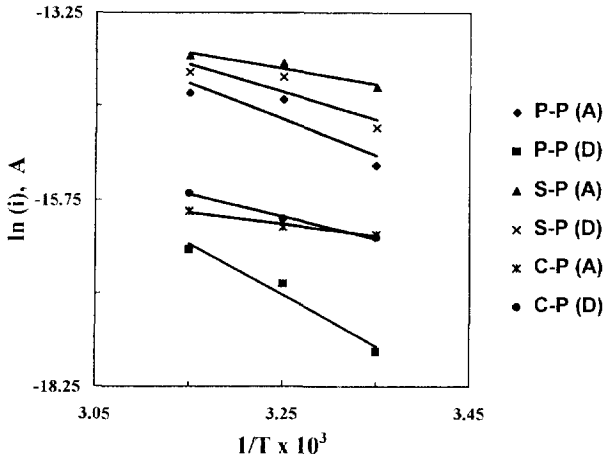

Fig. 5. Temperature dependence of the steady state photocurrent for photogalvanic cells in air-equilibrated (A) and deaerated (D) solutions.

At the dark electrode

$$e^- + P1 \rightarrow P1^{\cdot -} \quad (4)$$

$$P1^{\cdot -} + Fe^{3+} \rightarrow P1 + Fe^{2+} \quad (5)$$

These results are in accordance with previously studied [21,22] mechanically coated thin films containing polymer-bound zinc porphyrin systems. In contrast, in air-equilibrated solutions, the negative sign of the observed photocurrent suggests that P2 acts as a cathode and charge migration takes place through the medium.

In order to explain the change in polarity of the electrodes in air-equilibrated solutions, the redox properties of the thin film electrodes and the constituents in the medium were compared on the basis of cyclic voltammetric data. The excited state oxidation potential of the illuminated P2 thin film electrode has been calculated [23] as the sum of the electronic excitation energy and ground state redox potential, i.e. $E[P2^+/P2^*] = E[P2^*] + E_0[P2^+/P2]$, where the redox potentials indicated correspond to the reference electrode SCE [16]. It is found that the observed potential of the illuminated P2 electrode is +1.50 V, which indicates the formation of the porphyrin cation ($P2^{\cdot +}$). In air-equilibrated solutions, P2*, being a stronger reducing agent, reacts with molecular oxygen to give $P2^{\cdot +}$ and superoxide ion. Indeed, this is a thermodynamically favoured pathway, and the free energy [16,24] was calculated to be −0.81 eV using the equation $\Delta G = -E(P2^*) + e[E_{ox}(D) - E_{red}(A)]$, where the donor (D) is the P2 electrode and oxygen is the acceptor (A). It should be noted that the photoreduction of oxygen was reported by Memming and Schroppel [25] in PEC cells consisting of monolayer assemblies of stearoyl carboxy ester derivatives of $[Ru(bpy)_3]^{2+}$ deposited on a tin oxide electrode. Reduction of oxygen was also reported recently with phthalocyanines, zinc phthalocyanine films of dye embedded in poly(vinylidene fluoride) [26] and films on gold interdigitated microcircuit arrays [27]. It is therefore postulated that the photocurrent for the P–P cell in air-equilibrated solution arises from photoinduced electron transfer at the illuminated electrode.

The activation energy (ΔE) for the migration of the photogenerated charge carriers in P–P cells is estimated from the dependence of the short-circuit photocurrent (i) and temperature (T) as follows

$$i = A \exp(-\Delta E/kT) \quad (6)$$

where A and k are the pre-exponential factor and Boltzmann constant respectively. A linear relationship is observed

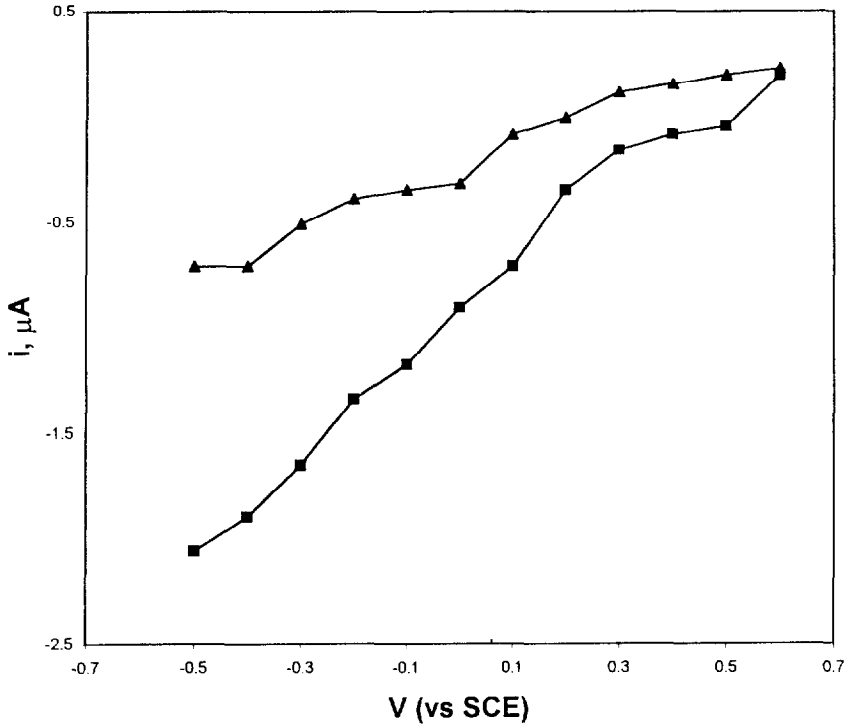

Fig. 6. Plot of the photocurrent vs. the applied voltage for P–P cell with Pt (■) or P1 (▲) electrode in the dark compartment.

between the reciprocal of T and log i in the range 298–318 K as shown in Fig. 5. The ΔE values for the P–P cells in air-equilibrated and deaerated solutions are found to be 0.41 and 0.59 eV respectively. These values are comparable with those reported [14,22] for polymer-bound zinc porphyrin or mechanically coated porphyrin thin film electrodes.

The photocurrent rectification behaviour for the P–P cell was examined in deaerated solution by applying a constant potential to the P2 electrode. A plot of the photocurrent i vs. the applied voltage V for the galvanic cell is shown in Fig. 6, where "i" is the difference between the dark and photoinduced currents at a particular applied potential. It shows a proportional increase in the photocurrent, a behaviour similar to that observed for vacuum-deposited thin film electrodes [28]. Marked rectification of the photocurrent is an apparent property for the platinum electrode, where the conduction resistance is much lower ($10.6\ \mu\Omega\ cm^{-1}$) [29] than that of ITO-coated glass ($4\ \Omega\ cm^{-1}$). In order to obtain information about the nature of the intermediates in the charge migration processes, the photocurrent was observed as a function of the wavelength of light used for irradiation of the P–P cell. Numerous results have been published in the literature [30] on the photovoltaic action spectra of cells constructed with organic compounds as photoactive species. The action spectrum of the P–P cell is shown in Fig. 7, which is very similar to the steady state UV–visible spectrum of P1.

3.3. Photoelectrochemical properties of electrode coated with sandwich thin films

The photovoltaic properties of the electrodes coated with sandwich polymer thin films were examined with the following (S–P) cell configuration

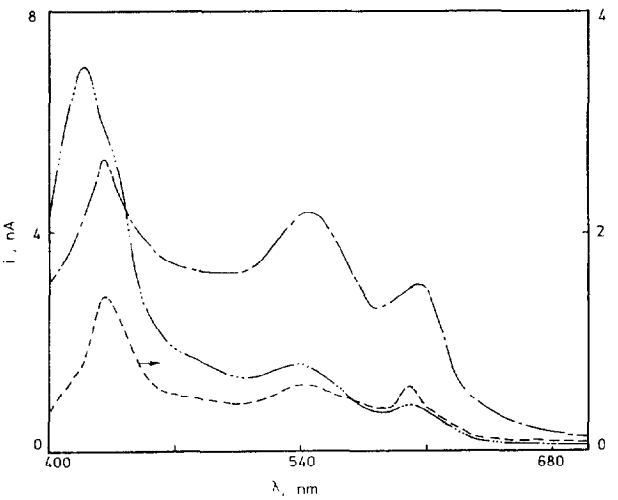

Fig. 7. Photocurrent action spectra for P–P (– – –), S–P (– · –) and C–P (– · · · –) cells in deaerated solution.

ITO(S1)/Fe(II) // Fe(III)/ITO(P1)

where S1 and P1 are the illuminated and dark electrodes respectively. The photocurrent response profile obtained during the light on/light off sequence is shown in Fig. 4(c). The observed photopotential (ΔE_{oc}) and short-circuit photocurrent (I_{sc}) (Table 2) indicate the operation of a charge transfer mechanism similar to that observed for the P–P cell. On illumination of the S–P cell, the charge migration and photocurrent generation in an air-equilibrated solution follow the photoassisted charge separation of $S1^{*+}$ and the reduction of oxygen, which is characteristic of negative photocurrent generation as described above. However, the presence of quinone polymer results in an increase in the photocurrent by a factor

of two. In deacrated solutions, the cell shows a behaviour corresponding to the mechanism proposed for the P–P cell, with a marginal increase in the photocurrent generation, which is presumably due to the large internal resistance of the coated electrode. Indeed, such an observation with reference to the internal resistance of the electrodes was observed in the case of porphyrin [14] and phthalocyanine [6] thin film-coated electrodes.

The activation energies determined for air-equilibrated and deaerated solutions in the S–P cells are 0.18 and 0.32 eV respectively (Fig. 5), smaller than those observed for the P–P cell. The reduction in activation energy is due to an increase in the migration of photogenerated charge carriers. The *i–V* characteristics for the S–P cell under deaerated conditions are shown in Fig. 8. Interestingly, this system shows a large cathodic current around −0.5 V, attributable to the reduction of the poly(AQP) film, indicating that the polymeric quinone thin film, which is separated by the polymer–porphyrin thin film from the film–solution interface, contributes to the generation of photocurrent together with the excited state of the porphyrin. A plot of the photocurrent as a function of the irradiation wavelength is shown in Fig. 7, which is similar to the absorption spectrum of monomeric ZnPOH in solution. Quinone alone shows no absorption in the visible region and therefore the photocurrent is obviously due to the absorption of light by ZnPOH. However, the intensity ratio of Soret/Q band is decreased due to the increasing Q band photocurrent generation, indicating an interaction between the singlet excited state of ZnPOH and quinone. The steady state absorption and emission properties described in the earlier sections do not suggest the formation of a complex, and hence the changes in the *i–V* curves and action spectra are attributed primarily to electron or energy transfer processes.

3.4. Photoelectrochemical properties of electrodes coated with thin films of copolymer

The photovoltaic properties of electrodes coated with thin films of copolymer (C1) were examined by illuminating C1 with P1 functioning as a dark electrode. The C–P cell configuration is shown below

ITO(C1)/Fe(II) // Fe(III)/ITO(P1)

The PEC characteristics of the cell, shown in Table 2, indicate that the pathways of charge migration and the nature of the species produced in the air-equilibrated and deaerated solutions are the same as in the P–P and S–P cells. However, the magnitude of the photocurrent generation under deaerated conditions increases three- to four-fold compared with that of the P–P and S–P cells. The activation energies under air-equilibrated and deaerated conditions are 0.25 and 0.13 eV respectively for the C–P cells (Fig. 5). The ΔE value for charge migration in air-equilibrated solution is comparable with that of other quinone-containing S–P cells, whereas it is much lower in deaerated solutions. The activation energy for air-equilibrated solution is lower than that for deaerated solution in P–P and S–P cells, whereas the reverse is true for C–P cells.

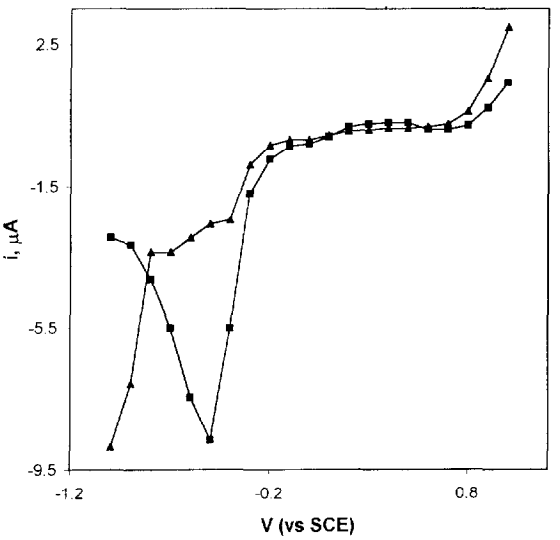

Fig. 8. Plot of the photocurrent vs. the applied voltage for S–P cell (■) and C–P cell (▲) in deaerated solution.

The photocurrent vs. applied potential plot for the C–P cells, given in Fig. 8, shows a large increase in the cathodic and anodic currents when the applied potential goes beyond −0.4 V and +0.8 V, presumably due to the reduction of the intercalated quinone with concomitant oxidation of the porphyrin moiety. The action spectrum (Fig. 7) for the C–P cells shows a similar behaviour to that of P–P cells. However, a relative increase in the photocurrent value is observed irrespective of the illumination wavelength, which may be due to the interaction of the excited state porphyrin with the intercalated quinone.

3.5. Comparative photovoltaic performance of modified electrodes

The photovoltaic cells consisting of modified ITO electrodes exhibit short-circuit photocurrents in the range −19nA to 650 nA and open-circuit photopotentials as high as 210 mV on illumination with a 150 W halogen lamp (Table 2). In all cases, the time taken to reach a steady state current is relatively low (less than 8 s) (Fig. 4). The morphology of the multilayer arrays on the electrode affects the energy transduction mechanism within the pigment and thus influences the overall charge migration of the cell. The presence of oxygen influences the nature of the electrode reactions. The overall behaviour for the air-equilibrated and deaerated solutions is found to be similar for all three cells (P–P, S–P and C–P), but the observed photocurrent and photopotential values are different. An increase in the photopotential and photocurrent was observed in the quinone-containing cells (S–P and C–P), which may be due to the additive or synergistic effect of the quinone moieties in the electrodes. In particular, deaerated C–P and air-equilibrated S–P cells show a somewhat higher photocurrent. All the photogalvanic cells show

a large amount of photorectification behaviour when a constant potential is applied to the electrodes. The *i–V* characteristics clearly demonstrate the interaction between the quinone and excited state porphyrin for S–P and C–P cells. In the case of the former, reduction of the poly(AQP) thin film and its interaction with the porphyrin excited state are observed at around −0.5 V, whereas in the C–P cell with the intercalated quinone reduction is not observed. Although the action spectra of the cells have similar characteristics to those of monomeric ZnPOH in solution, a moderate change in the Q band region for S–P cells suggests an interaction between quinone and the porphyrin excited state.

Acknowledgements

This work was partially supported by a DST-SERC Project. One of the authors (E.B.) acknowledges CSIR (EMR), New Delhi for providing a senior research fellowship.

References

[1] H. Meier, W. Albrecht, U. Tschirwitz, Angew. Chem. Int. Ed. Engl. 11 (1972) 1051. Z. Taha, T. Malinski, Nature 358 (1992) 676. T. Malinski, Z. Taha, S. Grunfield, A. Burewicz, P. Tomboulian, F. Kiechle, Anal. Chim. Acta 279 (1993) 135. I. Willner, R. Blonder, A. Dagan, J. Am. Chem. Soc. 116 (1994) 9365.
[2] S. Licht, N. Myung, Y. Sun, Anal. Chem. 68 (1996) 954.
[3] K.-Y. Law, Chem. Rev. 93 (1993) 449. D. Worhle, D. Meissner, Adv. Mater. 3 (1991) 129.
[4] A.J. Bard, Science 207 (1980) 139. H.T. Tien, J. Higgins, J. Electrochem. Soc. 127 (1980) 1475. B.O. Regan, M. Gratzel, Nature 353 (1991) 737. J. Basu, K.K. Rohatgi-Muherjee, Solar Energy Mater. 21 (1991) 317. Y.-S. Kim, K. Liang, K.-Y. Law, D.G. Whitten, J. Phys. Chem. 98 (1994) 984.
[5] T.J. Meyer, Acc. Chem. Res. 22 (1989) 163. A. Kay, M. Gratzel, J. Phys. Chem. 97 (1993) 6272.
[6] D. Wohrle, L. Kreienhoop, G. Schnurpfeil, J. Elbe, B. Tennigkeit, S. Hiller, D. Schlettwein, J. Mater. Chem. 5 (1995) 1819.
[7] R. Tamilarasan, P. Natarajan, Indian J. Chem. 20A (1981) 1149. R. Tamilarasan, P. Natarajan, Nature 292 (1981) 224. R. Tamilarasan, R. Ramaraj, R. Subramaniam, P. Natarajan, J. Chem. Soc., Faraday Trans. I 80 (1984) 2405. P. Natarajan, J. Macromol. Sci. Chem. A 25 (1988) 1285. R. Ramaraj, P. Natarajan, J. Chem. Soc., Faraday Trans. I 85 (1989) 813. K. Viswanathan, P. Natarajan, J. Photochem. Photobiol. A: Chem. 95 (1996) 255.
[8] R.W. Murray, Acc. Chem. Res. 13 (1980) 135. M. Kaneko, D. Wohrle, Adv. Polym. Sci. 84 (1988) 141. R.W. Murray, in: A.J. Bard (Ed.), Electroanalytical Chemistry, vol. 13, Marcel Dekker, New York, 1984, p. 191.
[9] A. Deronzier, J.-C. Moutet, Acc. Chem. Res. 22 (1989) 249. A. Bettelheim, B.A. White, S.A. Raybuck, R.W. Murray, Inorg. Chem. 26 (1987) 1009. T.J. Savenije, R.B.M. Koehorst, T.J. Schaafsma, Chem. Phys. Lett. 244 (1995) 363. F. Bedioui, J. Devynck, C. Bied-Charreton, Acc. Chem. Res. 28 (1995) 30.
[10] V. Balzani, F. Scandola, Supramolecular Photochemistry, Horwood, Chichester, 1991.
[11] T. Watanabe, A. Fujishima, O. Tatsuoki, K. Honda, Bull. Chem. Soc. Jpn. 49 (1976) 8.
[12] T. Malinski, A. Ciszewski, J. Bennett, J.R. Fish, L. Czuchajowski, Adv. Mater. 4 (1992) 354. G. Perrier, R. Gauthier, L.H. Dao, J. Electrochem. Soc. 135 (1988) 598.
[13] Y. Harima, K. Yamamoto, K. Takeda, K. Yamashita, Bull. Chem. Soc. Jpn. 62 (1989) 1458. E. Balasubramaniam, P. Natarajan, J. Photochem. Photobiol. A: Chem., 103 (1997) 201–211.
[14] K. Takahashi, K. Horino, T. Komura, K. Murata, Bull. Chem. Soc. Jpn. 66 (1993) 733.
[15] D.D. Perrin, W.L.F. Armarego, D.R. Perrin, Purification of Laboratory Chemicals, Pergamon, Oxford, 1981.
[16] E. Balasubramaniam, G. Ramachandraiah, P. Natarajan, C. Bied-Charreton, J. Devynck, F. Bedioui, J. Mater. Chem. 5 (1995) 625.
[17] R. Hiesgen, D. Meissner, Ultramicroscopy 42–44 (1992) 1403.
[18] F. Bedioui, M. Voisin, J. Devynck, C. Bied-Charreton, J. Electroanal. Chem. 297 (1991) 257.
[19] M. Gouterman, in: D. Dolphin (Ed.), The Porphyrins, Part A, vol. III, Academic Press, New York, 1978, p. 1.
[20] V.S.-Y. Lin, S.G. Dimagno, M.J. Therien, Science 264 (1994) 1105.
[21] A.M. Crouch, I. Ordonez, C.H. Langford, M.F. Lawrence, J. Phys. Chem. 92 (1988) 6058.
[22] M.F. Lawrence, Z. Huang, C.H. Langford, I. Ordonez, J. Phys. Chem. 97 (1933) 944.
[23] K. Kalyanasundaram, Photochemistry of Polypyridine and Porphyrin Complexes, Academic Press, London, 1992, p. 447.
[24] R. Memming, Electroanal. Chem. 11 (1979) 1.
[25] R. Memming, F. Schroppel, Chem. Phys. Lett. 62 (1979) 207.
[26] D. Schlettwein, M. Kaneko, A. Yamada, D. Wohrle, N.I. Jaeger, J. Phys. Chem. 95 (1991) 1748.
[27] J.W. Pankow, C. Arbour, J.P. Dodelet, G.E. Collins, N.R. Armstrong, J. Phys. Chem. 97 (1993) 8485.
[28] H. Yanagi, Y. Kanbayashi, D. Schlettwein, D. Wohrle, N.R. Armstrong, J. Phys. Chem. 98 (1994) 4760.
[29] R.C. Weast, M.J. Astle (Eds.), Handbook of Chemistry and Physics, CRC Press, Boca Raton, FL, 1979, p. E-85.
[30] A.K. Ghosh, D.L. Morel, T. Feng, R.F. Shaw, C.A. Rowe Jr., J. Appl. Phys. 45 (1974) 230. C.W. Tang, A.C. Albrecht, J. Chem. Phys. 63 (1975) 953. J.-P. Dodelet, H.-P. Pommier, M. Ringuet, J. Appl. Phys. 53 (1982) 4270. M. Khelifi, M. Mejatty, J. Berrehar, H. Bouchriha, Rev. Phys. Appl. 20 (1985) 511. A. Desormeaux, J.J. Max, R.M. Leblanc, J. Phys. Chem. 97 (1993) 6670.